Simplified stage construction and creep analysis of a segmental precast concrete bridge

A. Guarnieri, F. Bontempi & F. Petrini
University of Rome La Sapienza, Italy

ABSTRACT: In this work, a simplified methodology is developed for evaluating the evolution of strain/stresses or forces/deflections during the construction process of a segmental concrete precast bridge erected using a balanced cantilever method. The focus of the study is on modeling the entire construction process in stages (most significant) and the prestressing system, considering creep effects in a finite element model. During construction, the superstructure adopts a cantilever static scheme that change into a supported continuous beam upon the last stage. An original method for calculating creep phenomena has been implemented, involving the definition of a 'weighted' creep factor, which allows bypassing the limitations of the more common commercial codes in modeling such phenomena. Once the conceptual framework of the problem modeling is defined, it becomes possible to transfer all the acquired knowledge to more sophisticated models that use 2D or 3D elements and can address more complex local issues.

1 INTRODUCTION

For concrete bridges, the partition of the deck into segments becomes necessary for spans exceeding 50m, and the use of segments prefabrication proves to be a cost-effective solution in terms of launching equipment costs for long extensions and spans up to 120m. The construction methodology adopted in this work is well known as "Balanced Cantilever Method (BCM)" where the structure is erected by cantilevering through the initial construction of two cantilevers supported by an adequate prestressing system *Barras et al. (2003)*. The typical cross – sections used in this type of construction are single-cell or multi-cell box girder, appropriately equipped with upper and lower ducts for prestressing tendons and eventually deviators in the case of external post - tensioning *Suntharavadivel (2005)*. The static scheme can vary (with continuous beam or frames static schemes) depending on economic, environmental, and construction needs, but reference will be made here to the case of a continuous deck on multiple supports with a parabolic tapering (a suitable solution for spans greater than 70m). The BCM involves constructing the deck starting from the piers and symmetrically progressing cantilever-wise from both sides, progressively placing various segments (each ranging from 3 to 6 meters in length) until they meet in the midspan where closure occurs through the installation of a cast-in-place stitch segment (this process is applied to all central spans). The portion of the deck coming from the abutment, of shorter length, can be erected either using an asymmetric cantilever technique or can be temporarily supported by a provisional structure until the structural continuity of the bridge is restored. In prefabrication, the placement of segment pairs generally occurs every 7 days, and in the work presented here, prefabricated segments positioned using ground cranes will be considered: their use does not impose additional load on the structure during the segment placement phase, and the weight of the segment does not bear on it until they are fixed through temporary prestressing bars. Post - tension in the cantilever construction phase is applied to the top slab with a strong eccentricity to generate a bottom positive moment that counteracts the upper negative moment induced

by the self-weight in the cantilever diagram. At the end of construction, after the casting of the stitch segment, structural continuity will be restored by using post - tensioned continuity tendons, which can be placed either inside the bottom slab or internally within the box girder through external prestress. These tendons will be tasked with making the entire deck integral and providing a moment opposing that generated by permanent nonstructural and service loads. The use of segments also needs the restoration of shear continuity through "dry" joints *Petrangeli (1996)* that exploit the presence of "shear keys" between two successive segments. The use of shear keys is combined with the use of epoxy resins applied to the face of one of the two segments before temporary anchorage and, in addition to serving as a waterproofing function, can offer decent tensile strength during the construction stage *Shamass et al. (2016)*. In conclusion of this brief introduction, it is important to emphasize that one of the most significant aspects of this construction method concerns geometric issues *Petrangeli (1996)*, as cantilever lengths of different spans will have different vertical displacements. The investigation of differential displacements between the ends of the two cantilevers (the one from the abutment and the one from the pier) is crucial for designing initial elevations and any altimetric calibrations of the various segments to avoid misalignments during the casting of the stitch segment.

2 CASE STUDY

The proposed deck is sized from the beginning with reference to the spans that typically characterize this design solution, emphasizing that the focus of the study is not so much on the correct sizing of all structural elements and the search for the most economically advantageous solution but on the simplified procedure that can be implemented in many commercial and non-specific bridge finite elements software.

2.1 *Bridge description*

The structure consists of a continuous beam with three spans on four supports, featuring single-cell box girder with variable height, ranging from 5.0 m at the central support on piers to 2.0 m at the mid-spans (Fig. 1) through parabolic tapering. The initial construction stage involves erecting two symmetrical central cantilevers each of length 90.0 m and two side cantilevers each of length 18.0 m, employing cantilever diagram during construction stages (Fig. 1, left side). Subsequently, structural continuity will be restored through the casting of three stitch segments, each with a length of 0.60 m, and the insertion and prestressing of continuity tendons (Fig. 1, right side). The materials assumed involve the use of C40/50 class concrete and low-relaxation 7-wire stabilized strands with a diameter of 15.7mm (0.6") and Young's modulus E=201.000 MPa. In the conception of the cross sections *Florida Department of Trasportation (2002)*, consideration has been given to the space occupied by the strands, their respective anchorage plates *Tensa (2023),* and the possible tendon layout, in order to consider sections that could be as closely adherent to reality as possible. This is because the space requirements of the prestressing elements involve appropriate thickening that significantly increases the self-weight of each segment that must be considered.

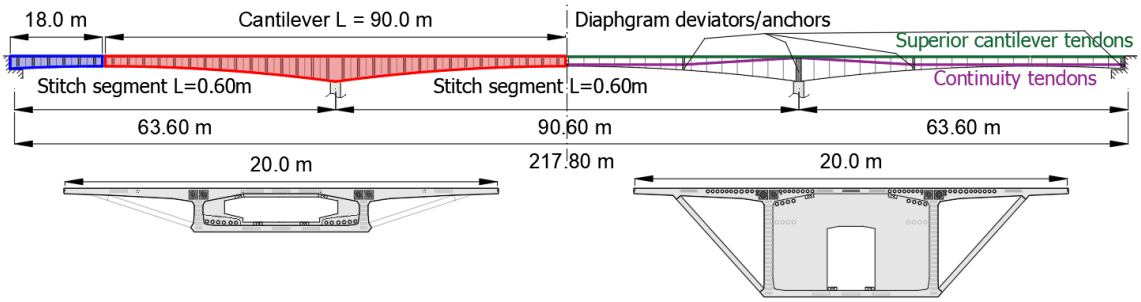

Figure 1. Longitudinal section of the bridge above, with the dimension of cantilever beams on the left and the disposition of tendons on the right. Below, the cross-section of the box girder, with the midspan section on the left (2.0 m deep) and the section on the piers on the right (5.0 m deep)

2.2 *Stage construction process*

Leaving aside the prefabrication phase, construction begins when the first segment is transported to the construction site, and lifting operations commence from below, placing it at the top of the piers using a crane or mobile crane. After positioning, altimetric calibration of the supports of the pier head segment is carried out, previously arranged on the pier, and a temporary fixed support is created using prestressed loop tendons to provide a certain rotational stiffness in case of load asymmetries. Successive pairs of segments are transported to the site, and before proceeding with the placement, an epoxy resin layer (with a working time of 1-2 hours and a drying time of about 1 hour) is applied to one of the two faces of each pair of conjugate segments (there are two pairs). Its purpose is to lubricate, waterproof, and possibly, with the use of specific resins, provide tensile capacity for the joints *Shamass et. al (2016)*. At this point, the pair of segments is positioned symmetrically on both sides of the structure. Using positioning bars passed through specific anchorage blisters, a temporary centered prestressing is applied to obtain a uniform compression of 0.2 – 0.3 MPa and allow the resin to take hold. After tensioning the positioning bars, the segment can support itself on the already constructed part of the structure, and the launching equipment can be released, allowing workers to proceed with the tendon placement operations. Once the resin has set, stressing of the upper prestressing tendons, previously inserted into the dedicated ducts in the upper slab, is carried out. If the resin used allows it, any tensile forces on the joint induced by the upper prestressing can be permitted during the construction stages, provided that the tensile strength of the concrete $\sigma_{t,limc}= 0.25 \cdot f_{ck}^{0.5}$ *Ministero delle Infrastrutture e dei Trasporti (2018)* is not exceeded. Once prestressing is complete, the positioning bars can be removed. If the resin does not allow for tensile stresses, temporary prestressing can be maintained until the lower continuity tendons are prestressed. This process is repeated for all subsequent segments to be inserted. Upon reaching the midspan of the span, it is necessary to create the closing segment that joins the decks coming from the two cantilevers (or from the abutments), making the bridge continuous. This is done by initially leaving a space of about 0.6 – 1.0 m between the last two segments and performing a cast-in-place pour. To connect the cantilever from the abutment with that from the pier, an altimetric correction of the supports must be provided before casting the stitch segment since, given the two different lengths, the displacements at the ends will be different. The last operation to be carried out in the construction stage is related to the stressing of the continuity tendons. These tendons will be positioned as the construction progresses and can be either internal (in which case they pass within the lower slab) or external (in which case they are placed inside the box and pass through deviators created with thickenings or actual diaphragms with variable thickness, usually from 0.4 to 1.0 m). Of these two configurations, modern construction techniques prefer the second because external post - tension (with tendons passing inside the box girder) allows for a complete inspection and repair in case of degradation, a critical aspect in post-tension with injected tendons *Suntharavadivel (2005)*. External post - tension also has the advantage of negligible friction losses, with the possibility of covering long distances with continuous tendons, as well as significant economic benefits in case of errors. It is advisable, during the prefabrication phase, to provide additional ducts in various deviators so that additional prestressing can be supplied over time if needed. During the construction, the bridge has fixed supports on piers and abutments, and at the end of the construction, a continuous beam over four support is reached with removal of temporary rotational constraints realized with the loop tendons mentioned above. In the upcoming analysis, the mentioned stages have been reproduced adopting appropriate simplifying assumptions:

1. Frictional phenomena are neglected, and bilateral tendons stressing is assumed
2. Relaxation and shrinkage effects are disregarded due to the use of stabilized strands and controlled 28-day curing (they can, however, be implemented in the procedure to be illustrated)
3. It is assumed that low tensile stresses are allowed during the construction stages
4. The effect of injecting the upper cables is neglected
5. A construction time of 98 days is considered (7 days for each pair of segments) for a total of 14 pairs, excluding the first one at the top of the piers
6. Each segment undergoes the initial loading step at an age of 28 days

Point 1 is considered plausible since the only tendons subject to friction are the upper ones. However, by introducing double side stressing, it ensures that both ends of the i-th pair of segments are subjected to the same compressive force. The occurrence of internal friction within the tendon does not affect the state of stress since the cable is pseudo-straight and does not have to transfer loads based on its curvature. Point 4 is considered plausible because the upper tendons primarily work during assembly to support the self-weight of the segments. The injection of these ducts, which occurs after the release of the beam's weight, does not provide substantial contributions to bearing additional loads, as these will be entirely supported by the continuity tendon.

3 FINITE ELEMENT MODEL AND ANALYSIS SETUP

The software used in this work is STRAND7©, which is not specific for bridge analysis. This paper aims to assist owners of this code or similar ones in the study of these types of bridges or similar structures, considering the possibly similar software limitations shown below. In STRAND7©, it is not possible to implement the evolution of creep phenomena (quasi static solver) simultaneously with the "assembly" of various elements in the non linear stage construction solver. Typically, what is done is taking the output of the stage construction solver and using it as an initial step for the creep analysis of the solver at each step. However, this approach tends to overestimate the effects of creep, as the load would be applied entirely in the initial step without considering the actual aging of concrete loaded at 7-day intervals. Importantly, it also does not account for the variation of boundary conditions after the first 98 days of assembly. This approach affects the initial tensile force to be given to the various tendons in the bridge design. An alternative procedure will be proposed to address these issues with good approximation while maintaining an acceptable solution accuracy.

3.1 *Phase 1 – Non linear construction stage analysis*

In the construction stage analysis *Zucca et al. (2018), Geethu (2016)* with STRAUS7©, it is possible to insert and/or remove elements and modify internal (link elements) or external constraint conditions during various construction stages, considering both geometric and material nonlinearities. The model used for this purpose involves the use of Beam-type elements (with flexural stiffness) for various segments and Truss-type elements (with only axial stiffness) to simulate the tendons. Since the tendons are eccentric, they are connected to the centroid of the Beam elements using rigid links. The tapering of segment elements and the behavior of sliding filaments in the tendons are achieved through the specific command now present in the majority of FEA software. Regarding the support conditions, a distinction is made between side cantilevers and central cantilevers. Side cantilevers lies directly on the abutment, and the support conditions will be simulated with a fixed support preventing vertical translation, horizontal translation, and rotation in the plane during the construction stage. Subsequently, after entering service, the external constraints on rotation and horizontal translation will be removed, simulating a roller support. It should be noted that the operation of removing external constraints can be performed on both solvers. For the central cantilevers, there is greater complexity due to the necessary presence of internal constraints (connection between pier and superstructure) that cannot be removed when transitioning from one solver to another. This modeling issue is addressed by using master-slave link elements for internal connections that do not change from the construction stage to service conditions. These link elements enforce the selected degrees of freedom to have the same displacements. In the case of the first pier-superstructure connection (chosen as a fixed point of the structure), relative horizontal and vertical translational displacements are fixed (hinge support). In the second connection, only the relative vertical displacement between abutment and superstructure is fixed (roller support). The simulation of the temporary rotational constraint during construction is introduced by inserting an external constraint that blocks rotation in the plane. In the real case, any bending moment generated by potential load asymmetries is countered by the flexural stiffness of the pier. In the assumed modeling, the rotational constraint is external and does not transmit bending actions to the pier. However, if the construction is executed correctly,

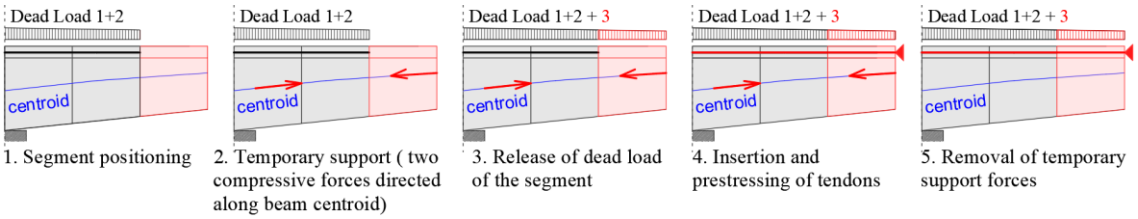

Figure 2. Modeling of the process from segment positioning to tendon stressing

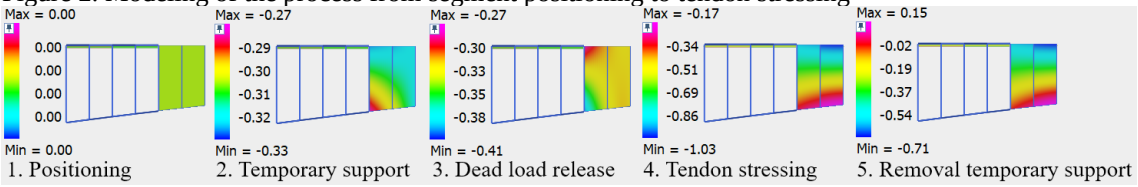

Figure 3 – Example of stage construction analysis for segment number three, stresses in MPa

these actions are not significant enough in this stage to explicitly require rotational continuity between the pier and the superstructure. The adopted simplification is deemed appropriate, and in service, the rotational constraint will be removed, restoring the hinge and roller behavior ensured by internal constraints. Having defined the boundary conditions, the next step was to define the construction stages that would be most critical for the controls on compressive and especially tensile stresses limits. Except for the first segment, a sequence of identical actions was defined for all subsequent segments until the casting of the stitch segment. The construction stages analysis begins with the placement of the first segment (beam element), assumed to be attached to the crane until prestressing occurs (resulting in zero self-weight on the structure). The upper prestressed tendon (truss element) is inserted, stressing is applied to the segment through an assigned pre-stress load on the tendon, and the crane is released (applying the self-weight to the structure). At this point, the first segment is positioned at the top of the pier (or abutment) and temporarily clamped with a fixed support. The placement of subsequent segments occurs similarly but with some additional steps. After placing the initial elements in stage zero, all subsequent ones will need to be placed on a deformed configuration compared to the initial modeling, with nodes of the model having undergone mutual displacements due to initial loads. This implies that, upon inserting additional elements in subsequent stages, these will be pre-deformed compared to the initially modeled configuration, introducing states of stress that are not real. To avoid this behavior, various software options provide more or less complex solutions. In the case of STRAUS7©, the morphing and rotate cluster options have allowed the insertion of elements into the deformed configuration with an initial rigid rotation equal to the rotation of the node to which the new element is attached, without introducing states of pre-stress. From the second segment onwards, the construction stages involve placing the segment on the structure (self-weight not yet acting), inserting temporary anchorages (this phase occurs immediately after applying epoxy resins, ensuring minimal compression and the ability to release the cranes), simulated by a load centered on the centroid of the newly inserted and the preceding element, releasing the self-weight, inserting and tensioning the upper prestressing tendons (Fig. 2). The process is repeated until the insertion of the stitch segment and the insertion of the continuity tendons, which, at the end of the staged analysis, will be inserted but unloaded. It is useful to repeat the analysis twice to evaluate the elastic differential vertical displacement that occurs between the ends of the cantilevers and assign this value as a positive vertical settlement of the hinge on the abutments, thus reproducing the altimetric calibration of the supports before the closure casting. Figure 3 illustrates the evolution of the stress state for the third segment.

3.2 *Phase 2 – Analysis of creep phenomena and long-term behavior*

The study of creep phenomena with STRAND7© *Tahmasebinia et al. (2019)* occurs by using the solution obtained from the staged solver as the initial input for the time-stepping analysis. Two issues need to be addressed: the first involves the variability of boundary conditions affected by

creep, starting with a cantilever scheme and eventually transitioning to a continuous beam scheme. The second arises from the solver constraint in which all loads from construction stages are applied from the initial step *Geethu (2016)*. The first problem is circumvented by observing that during the first 98 days of construction, creep phenomena tend to move the ends of the cantilevers away from those of the side spans with elongations of the stitch segment and the continuity tendon (this occurs only in the model since creep phenomena are introduced downstream of the construction and not during). As a result, a no-tension constitutive relationship is assigned to the three stitch segments, while the continuity tendon is assigned a zero elastic modulus, which will activate after 98 days along with its respective prestressing load. Once the time-stepping analysis is launched, in the first 98 days, the stitch segments will be non-reactive (concrete in tension); creep will act on the cantilever scheme. However, after 98 days, the entire elastic modulus, along with its corresponding tension load, is assigned to the continuity tendon. Temporary external constraints are removed by releasing rotations, resulting in the entire deck being compressed, just like the stitch segments, which, working in compression, contribute stiffness to the structural system. From this point onwards, all creep deformations and additional loads (permanent non-structural and service loads) will develop on the static scheme of a continuous beam over multiple supports. The second problem involves a significant overestimation of creep deformations. This aspect has led to the adoption of a methodology that will be explored in the following section, aiming to find a solution that still overestimates creep effects (underestimating them poses a significant challenge in older bridges) but minimizes the difference with the real solution as much as possible.

3.2.1 *Creep Analysis*

The creep model used for the analysis is that of UNI EN 1992-1-1 Appendix B. The creep coefficient is defined as:

$$\Phi(t_f, t_i)=\beta(t_f, t_i)\beta(t_i)\beta(f_{cm})\Phi_{RH}=\left(\frac{t_f - t_i}{\beta_H+(t_f - t_i)}\right)^{0.3}\cdot\frac{1}{0.1+t_i^{0.2}}\cdot\beta(f_{cm})\Phi_{RH} \quad (1)$$

where $\beta(t_f, t_i)$ represents the time development function starting from $t_f = t_i$ varying between 0 and approximately 1, while the remaining terms that depend on various factors (Relative Humidity %, mean compressive strength of concrete at 28 days f_{cm}, concrete age at the time of loading t_i, effective thickness h_0) provide the modulus of the creep function. The time and age dependence of the concrete at the time of loading are regulated by the first two terms. In nowadays software creep analysis is generally conducted through step-by-step analysis *Petrangeli (1996)*, which, for concrete matured for at least 28 days, is such that:

$$\varepsilon(t_f, t_i)=\frac{\sigma_0}{E_{28}}[1+\Phi(t_f, t_0)]+\sum_i\frac{\Delta\sigma_i}{E_{28}}[1+\Phi(t_f, t_i)] \quad (2)$$

The search for the exact solution through step-by-step integration requires that the various load steps $\Delta\sigma$ be introduced stage by stage with different concrete ages t_i for each element. However, using the already assembled superstructure as the initial step, the load is applied integrally and instantaneously. For instance, considering the first element, at the end of construction, the concrete age t_f will be 98 days + 28 days with $t_f - t_i = 98$ days. For the last element, t_f will be 0 days + 28 days with $t_f - t_i = 0$ days (construction is completed at the installation of the last element), while in this case, all elements will be evaluated at $t_f = 98$ days. To mitigate the overestimation of deformations resulting from such software limitations, the following approach is proposed:

$$\varepsilon(t_f, t_i)=\sum_i\frac{\Delta\sigma_i}{E_{28}}\left(1+\Phi(t_f, t_i)\right)=\frac{\Delta\sigma_{tot}}{E_{28}}\left(1+c\cdot\Phi\left(t_f, t_i^*, \beta_H^*\right)\right) \quad (3)$$

Setting aside the parameter ‘c’ (that is introduced only to scale creep coefficient Φ) for now, which will be used later, fictitious values for the age of the concrete at the first load 't_i' and the parameter ‘β_H’ are sought for each concrete element. These values are assigned to the various concrete elements during the analysis phase to enforce the equality of deformations (of the chosen control fibre) between the real curve that represent the correct strain evolution of the chosen control fibre according with (2) and the approximated one according with (3) at the point ‘t_f.’ If equality is assumed at infinite time, it is easily demonstrated that the influence of ‘β_H’ is null (and

therefore the real value will be used). The only parameter to be identified is 't_i^*', which can be obtained simply by reversing the expression for $\beta(t_i^*)$, as follows:

$$\beta(t^*) = \frac{\sum_i \beta(t_i)\Delta\sigma_i}{\Delta\sigma_{tot}} = \frac{1}{0.1+t^{*0.2}} \tag{4}$$

The use of this formulation, however, still leads to a certain overestimation of creep deformations compared to the real solution, coinciding with the approximate one only at infinite time.

A more complex approach involves applying (3) while varying the three parameters t_i, β_H and c, imposing a condition: the sum of the absolute percentage errors on deformations between the approximate curve and the real curve, evaluated at t_{fc} = 98 days, t_∞ = 10,000 days, t_a, and t_b, where the latter two are arbitrarily chosen points such that the first is close to t_{fc} and the second is a long-term value (>1000 days), is minimized. Through a target search using a simple spreadsheet, the point of minimum of the target function sum of errors $f_{\%}(t_i, \beta H, c, t_a, t_b)$ is sought, resulting in a curve that is closer to the real one. There is another possibility, not considered here as it strongly underestimates deformation compared to the real one, which involves imposing equality between the real and approximating functions at the end of the construction point t_{fc} as a function of the sole variable t^*. Although intuitive, it is essential to emphasize that the evolution of the stress state in terms of $\Delta\sigma_i$ is obtained from the stage analysis by choosing a control fiber (whose correct strain evolution is showed in Fig. 4 according with (2)) for each element, where the stress variation is acquired for use in equation (3). In addition, although the approximate solution is entirely incorrect from 0 to 98 days, this is of little importance since the critical conditions to be verified are the short-term ones (maximum stresses check) and the long-term ones (decompression). If these two conditions are verified, all those in between will also be satisfied. Figure 3-4 illustrate the real strain-time curves and those obtained through the three types of approximations seen earlier. With the defining curves for each element of the structure, it is possible to start the stepwise analysis, introduce permanent actions following the installation of the stitch segments and the tensioning of the continuity tendons, and study their effects over time. In this study, the creep coefficient weighted at infinite time was employed (Fig. 4 - 5 red curve), obtaining a response that overestimates creep deformations but was still considered plausible, having neglected the effects of steel relaxation and residual shrinkage after the 28-day curing period for each element. Figure 6 shows the evolution of vertical displacements and bending moments over time on the bridge in question. The purple arrows in Figure 6 (above) represent the differential displacement between the ends of the cantilevers and are zeroed by imposing a vertical settlement on the supports of the abutments, reproducing the previously mentioned altimetric calibration.

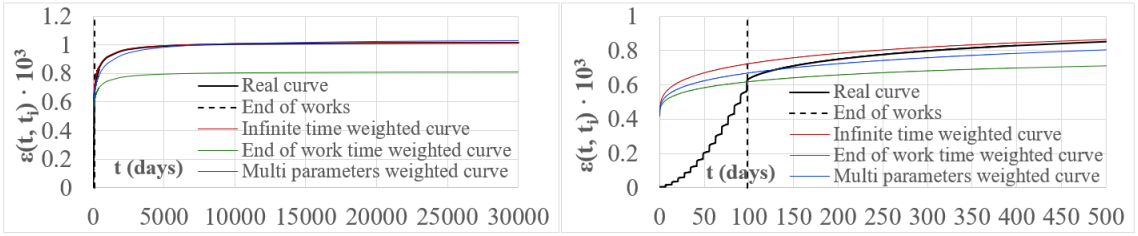

Figure 4. Strain – time curve comparison for segment 1, the multi parameter weighted curve was obtained with c = 0.985, t* = 85 days, β_H = 5628, t_a = 128 days, t_b = 5628 days

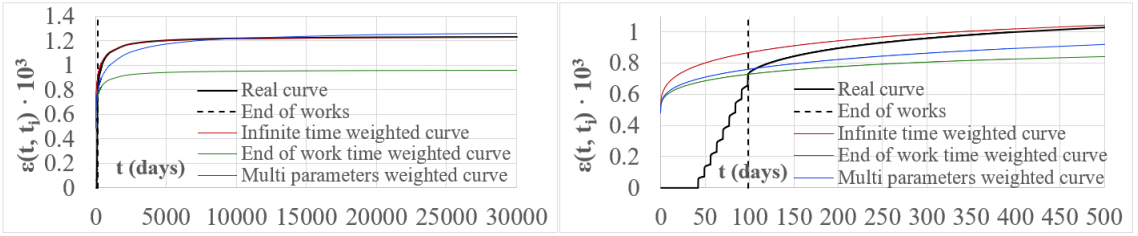

Figure 5. Strain – time curve comparison for segment 7, the multi parameter weighted curve was obtained with c = 0.967, t* = 41 days, β_H = 3245, t_a = 113 days, t_b = 7000 days

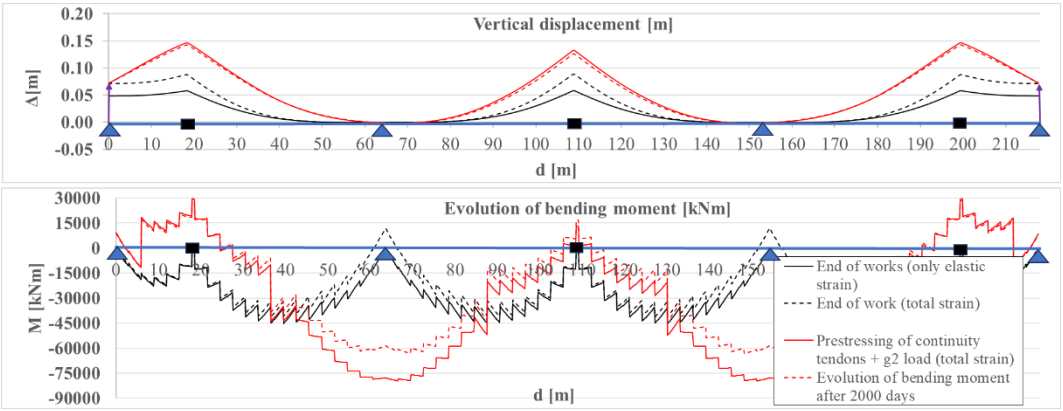

Figure 6. Evolution of vertical displacement (above) and bending moments (bottom) from 98d to 2000d

4 CONCLUSION

Through the adopted computational model for the study of this bridge, the global quantities involved in the construction of the deck during all construction stages were analyzed and evaluated. The purpose of the entire work was to understand the construction process of the specific bridge, distinguishing between negligible operations and those that must be considered and consequently analyzed. The next step was to translate these stages from reality to the FEA model, where an attempt was made to reproduce a sequence of actions and conditions that approached the real behavior as closely as possible. It is essential to understand how this work aims to lay the groundwork for a simplified modeling of bridge structures subject to non-negligible construction stages with creep effects. This allows for a good approximation of the evolution over time of bending moments and displacements (Fig. 6) even with non-specialized software. Although phenomena such as shrinkage and relaxation have been neglected in the model, there is nothing preventing their addition to the analysis, given the model's setup. Once the workflow is understood, it will be possible to transfer all the acquired concepts to more sophisticated models that use 2D or 3D elements, enabling the analysis of more complex issues such as local statics and kinematics, D-Regions, etc.

ACKNOWLEDGEMENT

This paper is derived from the master's thesis work of the first author under the supervision of the second and third authors.

REFERENCES

Barras, P., De Matteis, D., Derais, J., Duviard, M., Guillot, D., Lacombe, J., Lacoste, G., Lecointre, D., Ojeda, V., Paillusseau, P. & Reinhard, J. 2003. *Prestressed concrete bridges built using the cantilever method, Design guide*. Bagneux: Sétra

Florida Department of Trasportation 2002. *New Directions for Florida Post-Tensioned Bridges*. Tallahassee: Corven Engineering

Geethu, G. & Praseeda 2016. Comparison of Conventional and Construction Stage Analysis of a RCC Building. *International Journal of Science Technology & Engineering* 3(03)

Ministero delle Infrastrutture e dei Trasporti, CSLLPP 2018. *Norme tecniche italiane per le costruzioni.*

Petrangeli, M. 1996. *Progettazione e costruzione di ponti con cenni di patologia e diagnostica dei ponti esistenti, IV Edizione*. Milano: Casa Editrice Ambrosiana

Shamass, R., Zhou, X., Ph.D., M.ASCE & Wu, Z. 2016. Numerical Analysis of Shear-off Failure of Keyed Epoxied Joints in Precast Concrete Segmental Bridges. *Journal of Bridge Engineering* 22(1)

Suntharavadivel ,T.G. & Aravinthan, T. 2005. Overview of external post-tensioning in bridge. *Proceedings of the 2005 Southern Region Engineering Conference (SREC 2005)*. Toowoomba, Australia

Tahmasebinia, F., Fogerty, D., Wu, L., Li, Z., Sepasgozar, S., Zhang, K., Sepasgozar, S. & Marroquin, F. 2019. Numerical Analysis of the Creep and Shrinkage Experienced in the Sydney Opera House and the Rise of Digital Twin as Future Monitoring Technology. *Journal of buildings* 9(6)

Tensa Gruppo de Eccher, *Post-Tensioning datasheet.* Milano: Tensa

Zucca, M., Longarini, N., De Socio, F. & Migliori, I. 2018. Construction Stage Analysis for a New Mixed Structure Building in Milan. *International Journal of Structural Glass and Advanced Materials Research* 2(1): 66-72